[3] V. Tarokh, H. Jafarkhani, and A. R. Calderbank, "Space–time block coding for wireless communications: Performance results," *IEEE J. Sel. Areas Commun.*, vol. 17, no. 3, pp. 451–460, Mar. 1999.
[4] T. A. Tran and A. B. Sesay, "A generalized linear quasi-ML decoder of OSTBCs for wireless communications over time-selective fading channels," *IEEE Trans. Wireless Commun.*, vol. 3, no. 3, pp. 855–864, May 2004.
[5] A. Vielmon, Y. Li, and J. R. Barry, "Performance of Alamouti transmit diversity over time-varying Rayleigh-fading channels," *IEEE Trans. Wireless Commun.*, vol. 3, no. 5, pp. 1369–1373, Sep. 2004.
[6] D.-B. Lin, P.-H. Chiang, and H.-J. Li, "Performance analysis of two-branch transmit diversity block-coded OFDM systems in time-varying multipath Rayleigh-fading channels," *IEEE Trans. Veh. Technol.*, vol. 54, no. 1, pp. 136–148, Jan. 2005.
[7] P.-H. Chiang, D.-B. Lin, and H.-J. Li, "Performance analysis of two-branch space–time block-coded DS-CDMA systems in time-varying multipath Rayleigh fading channels," *IEEE Trans. Veh. Technol.*, vol. 56, no. 2, pp. 975–983, Mar. 2007.
[8] J. Kim, R. W. Heath, Jr., and E. J. Powers, "Receiver designs for Alamouti coded OFDM system in fast fading channel," *IEEE Trans. Wireless Commun.*, vol. 4, no. 2, pp. 550–559, Mar. 2005.
[9] X. Ma, G. Leus, and G. B. Giannakis, "Space–time-Doppler block coding for correlated time-selective fading channels," *IEEE Trans. Signal Process.*, vol. 53, no. 6, pp. 2167–2181, Jun. 2005.
[10] I. S. Gradshteyn and I. M. Ryzhik, *Table of Integrals, Series, and Products*, 5th ed. San Diego, CA: Academic, 1994.
[11] P. Bello, "Characterization of randomly time-variant linear channels," *IEEE Trans. Commun.*, vol. COM-11, no. 4, pp. 360–393, Dec. 1963.
[12] C. E. Shannon, "Communication in the presence of noise," *Proc. IRE*, vol. 37, pp. 10–21, 1949.
[13] L. Zheng and D. N. C. Tse, "Diversity and multiplexing: A fundamental tradeoff in multiple-antenna channels," *IEEE Trans. Inf. Theory*, vol. 49, no. 5, pp. 1073–1096, May 2003.
[14] R. U. Nabar, H. Bolcskei, and A. J. Paulraj, "Diversity and outage performance in space–time block coded Ricean MIMO channels," *IEEE Trans. Wireless Commun.*, vol. 4, no. 5, pp. 2519–2532, Sep. 2005.
[15] W. Su, Z. Safar, and K. J. R. Liu, "Diversity analysis of space–time modulation over time-correlated Rayleigh-fading channels," *IEEE Trans. Inf. Theory*, vol. 50, no. 8, pp. 1832–1840, Aug. 2004.

DPC-Based Hierarchical Broadcasting: Design and Implementation

Bin Liu, *Student Member, IEEE*,
Hongxiang Li, *Student Member, IEEE*,
Hui Liu, *Senior Member, IEEE*, and Sumit Roy, *Fellow, IEEE*

***Abstract*—This paper discusses interference precancellation in digital hierarchical broadcasting (HB). In particular, we present the principles and implementation of structured dirty paper coding (SDPC) that approaches the capacity limit of dirty paper coding in multilayer broadcasting. As an alternative to Tomlinson–Harashima precoding (THP), SDPC eliminates the significant performance loss suffered by THP in the low signal-to-noise ratio (SNR) regime due to the modulo operation. The key idea behind the SDPC scheme is the exploitation of the *modulation structure* of interference, thereby simplifying the demodulation process in hierarchical reception. We exemplify the SDPC technique by implementing an SDPC-based HB system on a real-time test bed. The experimental results show that SDPC delivers the performance of "superposition coding with successive interference cancellation" without extra computation or memory requirements at the receiver side.**

***Index Terms*—Dirty paper coding, hierarchical broadcasting, structured dirty paper coding, Tomlinson–Harashima precoding.**

I. Introduction

In digital TV or other wireless/wireline broadcasting applications, users at different locations will experience different channel qualities and signal strengths [1]. Ideally, users with better signal strength should be able to receive more information [e.g., high-definition TV (HDTV)] from the broadcasting source than those with lower signal strength (and, therefore, only the basic program). This can be achieved through the combination of source coding and hierarchical modulation [2]–[5]. The most commonly used hierarchical modulation scheme is hierarchical quadratic-amplitude modulation (QAM), where quaternary phase-shift keying (QPSK) carrying the first data stream is combined with another QAM carrying the second data stream, forming a multilevel superposition code [6]. The first QAM enables the basic program with a relatively low reception threshold, whereas the second QAM delivers additional information that can only be decoded at a higher reception threshold (for example, see Digital Video Broadcasting—Terrestrial (DVB-T) [1]).

While hierarchical QAM is intuitively simple, it suffers from some performance loss relative to regular QAM. The prime cause of the degradation is the cross interference between multiple data streams. To achieve the true channel capacity, superposition coding or hierarchical QAM with successive cancellation (HQAM-SC) must be employed to recover the loss in hierarchical QAM with independent demodulation (HQAM-ID). This inevitably leads to an extra cost that is sometimes prohibitive in both computation and memory at the receiver side.

Manuscript received December 29, 2006; revised September 8, 2007 and October 12, 2007. First published March 3, 2008; current version published November 12, 2008. The review of this paper was coordinated by Dr. C. Yuen.
B. Liu, H. Liu, and S. Roy are with the Department of Electrical Engineering, University of Washington, Seattle, WA 98105-2500 USA (e-mail: liub@u.washington.edu; huiliu@u.washington.edu; sroy@u.washington.edu).
H. Li was with the Department of Electrical Engineering, University of Washington, Seattle, WA 98105-2500 USA. He is currently with the Department of Electrical and Computer Engineering, North Dakota State University, Fargo, ND 58105 USA (e-mail: hongxiang.li@ndsu.edu).
Color versions of one or more of the figures in this paper are available online at http://ieeexplore.ieee.org.
Digital Object Identifier 10.1109/TVT.2008.919610

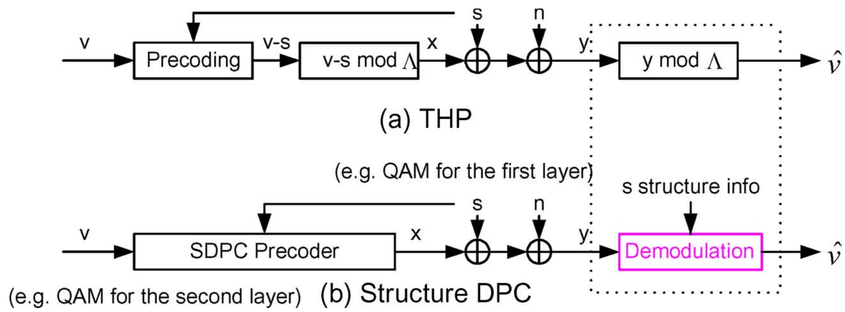

Fig. 1. (a) DPC implementation with THP. (b) DPC implementation with known interference structure.

Dirty paper coding (DPC) provides an intriguing alternative to receiver-end successive cancellation with interference precancellation at the transmission side [7]. Based on the results from Costa's groundbreaking paper in 1983, the capacity of a power-constrained channel with known interference is the same as that without interference. The hierarchical broadcasting (HB) situation can be precisely cast into a DPC framework, where multiple data streams are characterized as *known* interference to each other. The significant advantage of DPC over superposition coding, particularly in TV broadcasting, is that interference is presubstracted at the transmitter. Therefore, only independent decoding is needed to decode different data streams.

At a high signal-to-noise ratio (SNR), DPC can be approximated by Tomlinson–Harashima precoding (THP) [8], [9]. Unfortunately, THP has been shown to suffer from a 1.53-dB shaping loss in the high SNR regime [10]. In the low SNR regime, where broadcasting normally operates, the THP performance loss is even more significant, typically in the range of 4–5 dB [11]. The cause of this degradation is quantization (i.e., modulo operations) at the transmitter and the receiver. Several trellis precoding-based algorithms have been developed to recover the losses of THP [11], [14]. While in principle these algorithms can be applied to HB, the added complexity makes them less desirable in broadcasting applications.

Motivated by the promises of DPC and HB, this paper discusses DPC-based HB. Our focus is on the design of low-cost high-performance DPC techniques that can be used in practical broadcasting systems. In particular, we seek to develop low-complexity approaches that can reduce or eliminate the modulo loss at a low SNR. Toward this end, we observe that in most communication systems [e.g., wireless broadcasting and vector Digital Subscriber Line (DSL)], the interference structure is available to all receivers. Exploiting this known structure, we arrive at a new precoding algorithm [dubbed structured DPC (SDPC)] that reduces the modulo loss without undue complexity. Unlike the prior work that assumes *arbitrary* interference, SDPC takes advantage of the QAM structure of interference to achieve the DPC channel capacity with demodulation complexity similar to that of a regular QAM demodulator.

Another contribution of this paper is the realization of *SDPC-based HB* on a real-time test bed. This paper describes the implementation architecture of SDPC and the practical aspects of the broadcasting system. The performance of the real-time system is shown to be within 2 dB of the DPC additive white Gaussian noise (AWGN) capacity, with a data rate of up to 50 Mb/s on a field-programmable gate array (FPGA) test bed platform.

The rest of this paper is organized as follows: In Section II, we review the background and formulate the problem for broadcasting with known interference structure. The performance of DPC-based HB is compared with that of hierarchical QAM. In Section III, the SDPC precoding strategy is described. In Section IV, the bit error rate (BER) is analyzed, and numerical results are presented. The SDPC test bed and its performance are introduced in Section V. Finally, a conclusion is drawn in Section VI.

II. DPC and HB

A. DPC

DPC was introduced by Costa in [7]. In Fig. 1(a), an AWGN channel is corrupted by interference s, which is noncausally known at the transmitter. The source output v is the input to the precoder, whose output x obeys the transmitter power constraint: $E|x|^2 \le P_x$. Interference s and noise are assumed to be Gaussian independent identically distributed. P_n is the power of noise. Costa's result shows that the capacity of this channel is the same as if interference were absent, i.e., $C_{\rm DPC} = (1/2)\log(1 + (P_x/P_n))$.

In the high SNR regime, DPC can be approximated by THP [15]. THP was originally introduced in the context of ISI channel [8], [9]. The basic idea is illustrated in Fig. 1(a). In the first stage, interference s is directly subtracted from source v to compensate the interference in the channel. However, the power of $v - s$ may exceed the transmitter power constraint. A modulo operator is applied to enforce the power constraints at the transmitter. The quantizer level Λ is chosen to meet the power constraints without causing any ambiguity in v. At the receiver, another modulo operation is performed to recover the intended message v.

In [10], the capacity of the THP channel is shown to be

$$I(\hat{v}; v) = h\left((v + n) \bmod \Lambda\right) - h(n \bmod \Lambda). \tag{1}$$

In other words, the capacity of the THP channel is strictly less than the capacity of the corresponding DPC channel. In [17], the performance losses of THP are categorized into three classes: a shaping loss [14]–[16], a modulo loss [11], and a power loss. In this paper, we focus on the recovery of the most significant modulo loss in the low SNR regime.

The modulo loss is caused by the modulo operations at the THP system. Due to noise corruption, the signal at the boundary of the QAM constellation may be folded into the opposite side of the constellation, which incurs a potential error that would not have happened in a regular AWGN channel. The modulo loss is significant for low-order constellations in the low SNR regime (up to 3–4 dB). For the broadcasting applications of interest, the dominant loss is the modulo loss in the low SNR regime. One of the solutions is described in [12], where a statistical decoding method is used at the receiver to reduce the modulo loss in DPC. In the ensuing sections, we describe the SDPC principles that will eliminate the modulo loss all together. We focus our studies in low-order constellations (e.g., binary phase-shift keying and QPSK) since the high-order QAMs cannot operate in the low SNR regime.

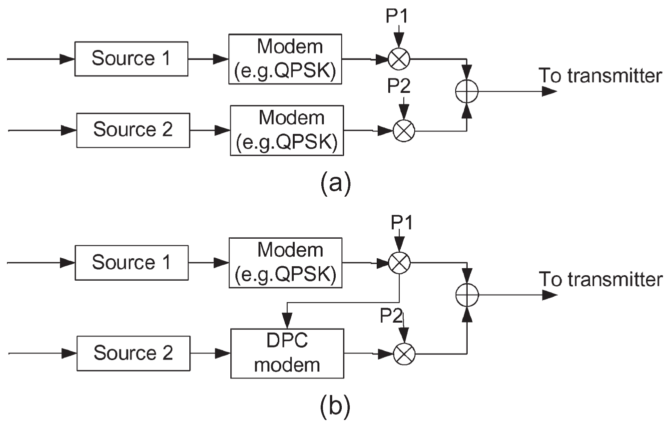

Fig. 2. (a) Hierarchical modulation with two signal sources. (b) DPC-based hierarchical modulation.

B. DPC in HB

Hierarchical QAM is an effective means to deliver multiple layers of source information to users experiencing different channel qualities. Fig. 2(a) illustrates the existing approach for hierarchical multimedia delivery. The two data streams (sources 1 and 2) are independently coded and modulated using QAM with power set to be P_1 and P_2, respectively. The two modulated signals are then mixed before being transmitted. Clearly, the two modulated signals will interfere with each other, leading to a certain performance loss at the receiver end.

At the receiver side, a user with low signal strength simply demodulates the basic signal (source 1), whereas users with higher signal strength can demodulate both sources 1 and 2 from the constellation. In particular, the signal received at the user end is given by

$$u = P_1 s_1 + P_2 s_2 + n \tag{2}$$

where n is the noise term. The achievable data rate of the first data stream is R_1. At a different location where the noise strength is weaker, the second data stream (with rate R_2 and a higher reception threshold) can independently be decoded as

$$R_1 = B \log\left(1 + \frac{P_1}{Bn_1 + P_2}\right) \tag{3}$$

$$R_2 = B \log\left(1 + \frac{P_2}{Bn_2 + P_1}\right) \tag{4}$$

where B is the channel bandwidth, and n_1 and n_2 are the power spectrum densities of the noise.

Note that in theory, s_1 can be decoded first and then subtracted from the received signal u before s_2 is demodulated. With such successive decoding, a higher rate can be achieved for s_2, i.e.,

$$R_{2,\mathrm{succ}} = B \log\left(1 + \frac{P_2}{Bn_2}\right). \tag{5}$$

Unfortunately, for successive cancellation, the receiver must first decode and store the "interference" and then cancel it out before decoding the signal of interest. In addition, a decoding delay will occur in s_2 demodulation. This is often impractical, given the large data block size and the high data rate in broadcasting.

The DPC principles can readily be applied to HB. With DPC, it is possible to jointly modulate multiple-source signals at the transmitter to allow interference-free reception. Such a design places the computational burden at the transmitter and significantly lowers the receiver cost at the user ends. Since data streams can independently be decoded, there will be no excessive memory requirement or decoding delay as in the case of successive demodulation. Specifically, in this scheme, the first data stream s_1 is modulated with a regular modem technique such as QPSK. Instead of independently generating the second signal, the interference from the first data stream is presubtracted using the DPC technique, as shown in Fig. 2(b). The second modulated data stream will suffer no interference from s_1 when reaching a receiver. As a result, the achievable data rate of the second stream is

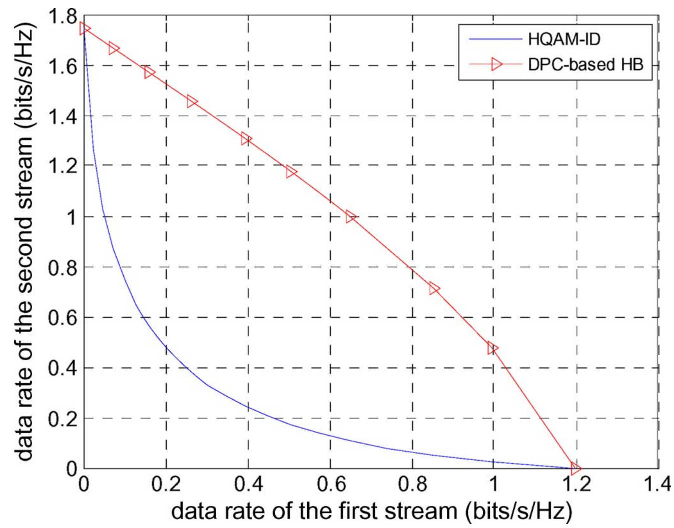

Fig. 3. DPC compared with the hierarchical modulation without successive cancellation at the receiver.

$$R_{2,\mathrm{DPC}} = B \log\left(1 + \frac{P_2}{Bn_2}\right) \tag{6}$$

which is identical to $R_{2,\mathrm{succ}}$ with a much complicated successive receiver structure. At the receiver, two data streams are independently decoded without interaction between the two demodulators. Consequently, there is no decoding delay.

The achievable rates of HQAM-ID and DPC-based HB are compared in Fig. 3. In this illustration, we assume that $P/n_1 = 10$ dB, $P/n_2 = 15$ dB, and $P = P_1 + P_2$. With the data rate of the first stream fixed, DPC-based HB has a much higher data rate for the second stream than that of HQAM-ID at the receiver.

III. Structured DPC

As mentioned in Section II, THP implementation of DPC will suffer from a performance loss of 4–5 dB in the low SNR regime [11]. A more efficient scheme must be developed to achieve the promise of DPC-based HB. In this section, we present the new approach (i.e., SDPC) that reduces or eliminates the modulo loss for pragmatic DPC implementation without undue complexity.

A. System Model

SDPC is motivated by the following observation. In scenarios such as wireless broadcasting and vector DSL, the modulation schemes of each layer (for different users) are sent over a control channel. In other words, each user knows the modulation schemes of all the layers. For example, in Fig. 1(b), v is the second-layer signal for user A, whereas s is actually the first-layer signal for user B. It is reasonable to assume that user A knows the modulation scheme of the first-layer signal intended for user B. We will show that this knowledge allows us to reduce (even eliminate in some cases) the modulo loss with proper precoding.

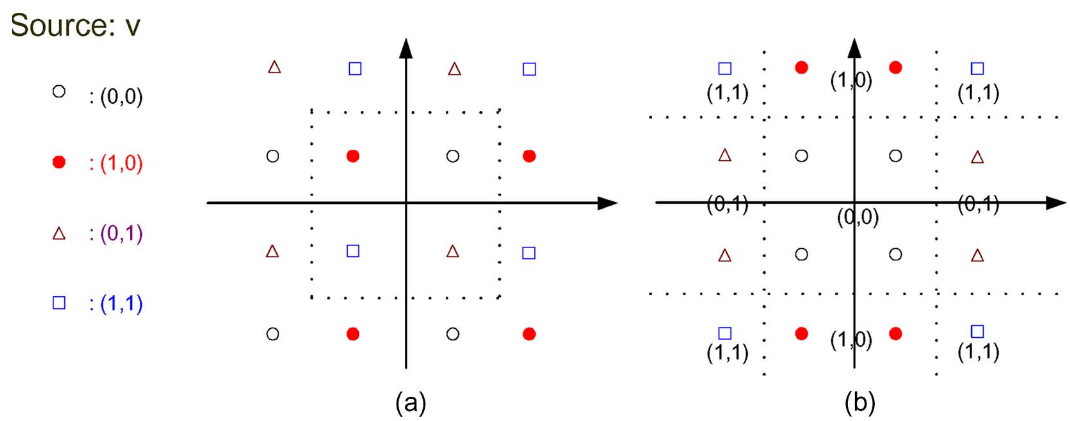

Fig. 4. (a) Constellation of y at the THP receiver. (b) Constellation of y at the SDPC receiver with QPSK source and interference.

B. Precoding With Known Interference Structure at the Receiver

As shown in Fig. 1(b), the receiver has prior knowledge of the constellation of y if s is a QAM interference. We also notice that the constellation of y at the THP receiver is generally an expanded version of the constellation of v due to the modulo operation at the transmitter. As a result, we should be able to directly demodulate y based on its constellation without performing the modulo operation as in THP. Along the same line, if we take advantage of the structure information of interference and accordingly design the precoder, a more receiver-friendly y constellation can be achieved.

The exact operation of SDPC in QPSK is described next.

1) Two Users With a QPSK Constellation: Since only low-order constellations are feasible in the low SNR regime, both signals are assumed to be QPSK. The different types of dots in Fig. 4 represent different source symbols at the receiver end. Fig. 4(a) can be viewed as the constellation of y at the input of the THP receiver. The received signal is folded (modulo) into a dashed box before performing detection at the THP receiver.

In the SDPC system, source information is directly demodulated from y using region-based (minimum distance) detection. Interestingly, we can rearrange the constellation of the received signal y for better performance through the SDPC precoder. It can be verified that the mapping shown in Fig. 4(b) yields the best performance. In fact, its BER performance is comparable with that of QPSK with the same minimum distance. Then, the SDPC precoding rule is accordingly designed.

a) *Precoding:* The precoder modulates 2 bits/symbol based on the following rule:

$$\begin{cases} x = v - s, & |v| > |s| \\ x = \mathrm{sign}(s)\,(|2i\cdot v - |v||) - s, & i = \left\lfloor \frac{1}{2}\left(\frac{|s|}{|v|}+1\right)\right\rfloor \\ & |v| \le |s|. \end{cases} \tag{7}$$

Here $|\cdot|$ denotes the amplitude, and $\lfloor\cdot\rfloor$ is the floor operator. The precoding rule is applied to both dimensions of the QPSK signal. The power of x is the average power of random signals $\pm[2(i-1)\cdot|v| - |s|]$ and $\pm[2(i+1)|v| - |s|]$, which are bounded.

b) *Decoding:* The decoder detects the 2-bit symbol based on the location of the received signal (relative to four decision regions). For $|v| > |s|$, the decision regions are the same as that of QPSK. For $|v| \le |s|$, the four decision regions are asymmetric, as illustrated in Fig. 4(b). Nevertheless, a direct mapping from source v to y can be established. By removing the *modulo operation*, the noise folded into the modulo interval around the origin is eliminated.

IV. Performance Analysis and Numerical Results

In this section, we analyze the performance of SDPC and present some numerical results.

A. BER Performance

First, we analyze the BER of the SDPC scheme and compare it with regular THP with dither. For QPSK signals with Gray labeling, the BER of THP, SDPC, and AWGN are calculated as follows:

$$P_{\mathrm{THP}} = 4 \times P_e/2 = \mathrm{erf}\,c\left(\sqrt{\frac{E_{b\_\mathrm{THP}}}{N_0}}\right) \tag{8}$$

$$P_{\mathrm{SDPC}} = 2 \times P_e/2 = \frac{1}{2}\,\mathrm{erf}\,c\left(\sqrt{\frac{E_{b\_\mathrm{SDPC}}}{N_0}}\right) \tag{9}$$

$$P_{\mathrm{AWGN}} = 2 \times P_e/2 = \frac{1}{2}\,\mathrm{erf}\,c\left(\sqrt{\frac{E_{b\_\mathrm{AWGN}}}{N_0}}\right) \tag{10}$$

where E_{b_THP}, E_{b_SDPC}, and E_{b_AWGN} are the average bit power, respectively.

Under the same transmitter power constraint, it is clear that

$$E_{b\_\mathrm{THP}} \le E_{b\_\mathrm{SDPC}} \le E_{b\_\mathrm{AWGN}}. \tag{11}$$

B. Numerical Results

Simulation studies have been conducted to validate the SDPC performance. In all simulations, THP with minimum mean square error scaling [18] is used as the baseline, and α is set at $P_x/(P_x + P_N)$. In our setup, the source and interference are both QPSK signals, and $|s| = 7.5|v|$. (SDPC can work at any ratio.) It is worth noticing that the SDPC gain is more significant when $|s|$ and $|v|$ are close to each other. SDPC has an about 1-dB power loss in this case. The results (theoretical versus simulation) are shown in Fig. 5. As shown, the curves very well match the theoretical predictions in (8)–(10).

We also run simulations to study the performance of SDPC with channel coding. A rate-1/2 (7, 5) turbo code is used with the log-MAP decoding algorithm. Eight iterations are performed in the turbo decoder. The results in Fig. 6 show that SDPC has more than 3-dB improvement over regular THP (with dither) in the low SNR regime.

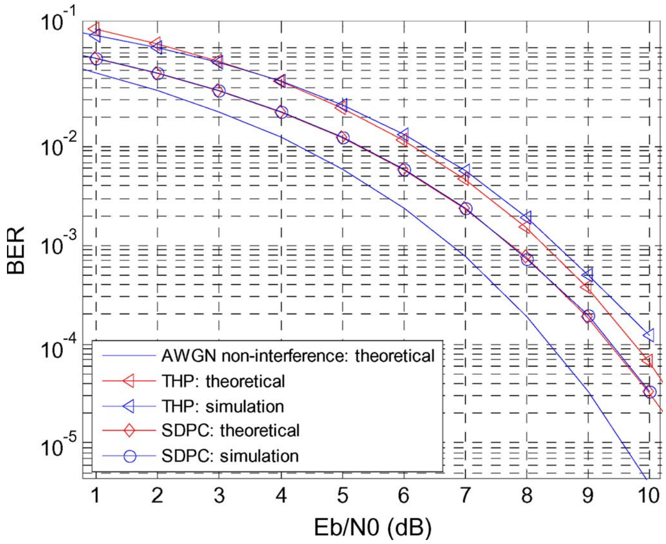

Fig. 5. BER versus E_b/N_0 for QPSK source and interference signals.

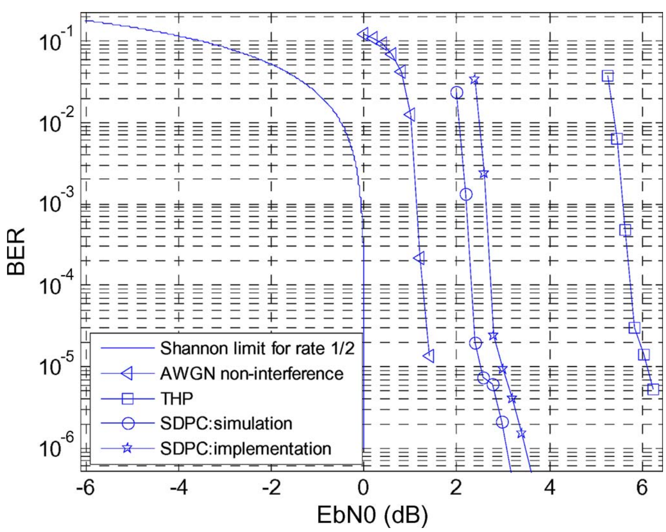

Fig. 6. BER versus E_b/N_0 with a rate-1/2 (7, 5) turbo code for QPSK source and interference signals.

The performance loss compared with the AWGN channel is less than 1 dB, which is due to the power loss.

The SDPC gain will diminish with large constellations—this is because the modulo loss is much smaller for high-order constellations.

V. SDPC Implementation

The principles of DPC-based HB is validated in real time at the Wireless Information Technology Laboratory, University of Washington. We describe SDPC implementation on an FPGA-based test bed in this section.

A. Test Bed Description and Decoder Architecture

The SDPC demo system is implemented on an SMT8036 development platform. SMT8036 is a complete development suite, which is hosted on an SMT310Q PCI carrier in a PC, for the evaluation of SMT365-4-2 and SMT370-AC modules. In particular, SMT365-4-2 has a Xilinx Virtex-II 2000 FPGA and a Texas Instruments' digital signal processor (DSP) TMS320C6416 on board. The Xilinx Virtex-II 2000 FPGA has about a 2 million system gates. The DSP runs at a 600-MHz system clock with 4800 peak million multiply–accumulate operations.

TABLE I
System and Performance Comparison

	HQAM-ID	HQAM-SC	SDPC-based HB
Max Throughput	$50Mbps$	$< 25Mbps$	$50Mbps$
Delay	/	$\approx 2.7ms$	/
Data Memory	/	$\approx 6Kbytes$	/
required E_b/N_0	$4.5dB$	$2.2dB$	$2.2dB$

In our demo system, the MPEG data stream is generated by an MPEG encoder, which resides in a PC. The MPEG data stream is fed into the SMT8036 platform through a parallel interface, called Sundance High-speed Bus. In our demo, the data rate of the MPEG bit stream is set at 5 Mb/s.

Within the SMT8036 platform, the MPEG data stream is processed in the FPGA before transmission. The data stream is first channel encoded with a rate-1/2 (7, 5) turbo encoder. The SDPC precoder follows the channel encoder, and the interference is a second coded MPEG source stored in the PC. For convenience, the interference bit rate matches the MPEG bit rate at 5 Mb/s.

The encoded signal and the interference are converted to an intermediate frequency (IF) signal centered at 70 MHz. Then, the SDPC encoded signal and the interference are mixed together before being looped back into the development platform. In the process, the signal is contaminated by AWGN noise.

At the receiver end, the IF signal is sampled and then sent into the FPGA, where SDPC decoding is conducted. Afterward, the data are transferred into the DSP for channel decoding, where a turbo decoder with the log-MAP decoding algorithm is implemented. Finally, the data are recovered and sent to an MPEG decoder. The video is displayed on a monitor.

B. Implementation Results

The performance of SDPC-based HB, HQAM-ID, and HQAM-SC is compared in our demo system. Since there is no difference in the demodulation for the first-layer data stream, the comparison is based on the demodulation for the second-layer data stream.

Given the available process power, the throughput of the SDPC-based HB system can reach 50 Mb/s. As shown in Fig. 6, the implementation loss is within 0.5 dB relative to the simulation results. We compare the SDPC-based HB and HQAM-SC systems on the same demo system. The HQAM-SC scheme requires a large data buffer for successive cancellation at the receiver end. In addition, since it must first demodulate the interference (i.e., the first data stream) for successive cancellation, the computational requirement is about two times, relative to SDPC-HB. The maximum achievable data rate on the test bed is reduced to 25 Mb/s. The simple HQAM-ID scheme, on the other hand, has a significantly higher reception threshold compared with SDPC-based HB and HQAM-SC.

Table I highlights the system and performance parameters of the three schemes. We choose a typical DVB-T setup [19] (the 2K mode), where both the first- and second-layer data are QPSK modulated. For both layers, the inner code is a rate-1/2 convolutional code, and the outer code is a Reed–Solomon code (204, 188). The code block size is 3264 bits. The maximum throughput is the data rate allowed by the demo system hardware. HQAM-SC has an approximate 2.7-ms delay and requires a 6-kB buffer (assuming word length of 16 bits) at the receiver side.

VI. Conclusion

In this paper, we have studied a low-cost DPC scheme for HB applications. For DPC implementation, the traditional THP approach suffers from a 3- to 4-dB modulo + power loss, which makes it unsuitable for HB with low-order constellations. The new SDPC method recovers most of the modulo loss without added complexity at the receiver side. In QPSK cases investigated, SDPC achieves a 2- to 4-dB improvement over regular THP (with dither). We have realized a real-time SDPC-based HB prototype that achieves the performance of HQAM-SC but with much lower complexity and no extra buffer requirement.

References

[1] *Eur. Telecommun. Stand. Inst. (ETSI) Digital Video Broadcasting (DVB)*, Nov. 2004.

[2] T. Cover, "Broadcast channels," *IEEE Trans. Inf. Theory*, vol. IT-18, no. 1, pp. 2–14, Jan. 1972.

[3] K. Ramchandran, A. Ortega, K. M. Uz, and M. Vetterli, "Multiresolution broadcast for digital HDTV using joint source/channel coding," *IEEE J. Sel. Areas Commun.*, vol. 11, no. 1, pp. 6–23, Jan. 1993.

[4] M. J. Hossain, P. K. Vitthaladevuni, M.-S. Alouini, and V. K. Bhargava, "Hierarchical modulations for multimedia and multicast transmission over fading channels," *IEEE Trans. Inf. Theory*, vol. 51, no. 1, pp. 154–172, Jan. 2005.

[5] A. Schertz and C. Weck, "Hierarchical modulation—The transmission of two independent DVB-T multiplexes on a single frequency," *EBU Tech. Rev.*, pp. 1–13, Apr. 2003.

[6] A. Goldsmith, *Wireless Communications*. New York: Cambridge Univ. Press, 2005.

[7] M. Costa, "Writing on dirty paper," *IEEE Trans. Inf. Theory*, vol. IT-29, no. 3, pp. 439–441, May 1983.

[8] H. Harashima and H. Miyakawa, "Matched-transmission technique for channels with intersymbol interference," *IEEE Trans. Commun.*, vol. COM-20, no. 4, pp. 774–780, Aug. 1972.

[9] M. Tomlinson, "New automatic equaliser employing modulo arithmetic," *Electron. Lett.*, vol. 7, no. 5, pp. 138–139, Mar. 1971.

[10] R. D. Wesel and J. M. Cioffi, "Achievable rates for Tomlinson–Harashima precoding," *IEEE Trans. Inf. Theory*, vol. 44, no. 3, pp. 824–831, Mar. 1998.

[11] W. Yu, D. P. Varodayan, and J. M. Cioffi, "Trellis and convolutional precoding for transmitter-based interference presubtraction," *IEEE Trans. Commun.*, vol. 53, no. 7, pp. 1220–1230, Jul. 2005.

[12] C. Yuen and B. M. Hochwald, "How to gain 1.5 dB in vector precoding," in *Proc. IEEE Globecom*, San Francisco, CA, 2006, pp. 1–5.

[13] A. Cohen and A. Lapidoth, "The Gaussian watermarking game," *IEEE Trans. Inf. Theory*, vol. 48, no. 6, pp. 1639–1667, Jun. 2002.

[14] U. Erez, S. Shamai, and R. Zamir, "Capacity and lattice-strategies for cancelling known interference," in *Proc. ISITA*, Honolulu, HI, Nov. 2000, pp. 681–684.

[15] R. Zamir, S. Shamai, and U. Erez, "Nested linear/lattice codes for structured multiterminal binning," *IEEE Trans. Inf. Theory*, vol. 48, no. 6, pp. 1250–1276, Jun. 2002.

[16] D. D. Forney, Jr., "Multidimensional constellations—Part I: Introduction, figures of merit, and generalized cross constellations," *IEEE J. Sel. Areas Commun.*, vol. 7, no. 6, pp. 877–892, Aug. 1989.

[17] S. Shamai and R. Laroia, "The intersymbol interference channel: Lower bounds on capacity and channel precoding loss," *IEEE Trans. Inf. Theory*, vol. 42, no. 9, pp. 1388–1404, Sep. 1996.

[18] U. Erez and S. T. Brink, "Approaching the dirty paper limit for canceling known interference," in *Proc. 41st Annu. Allerton Conf. Commun., Control, Comput.*, Oct. 1–3, 2003, pp. 799–808.

[19] U. Reimers, *Digital Video Broadcasting (DVB); The International Standard for Digital Television*. Berlin, Germany: Springer-Verlag.

Performance Prediction for Energy Detection of Unknown Signals

J. Eric Salt, *Member, IEEE*, and Ha H. Nguyen, *Senior Member, IEEE*

***Abstract*—This paper analyzes the energy detector that is commonly used to detect the presence of unknown information-bearing signals. The algorithm simply compares the energy (or power) in a sliding window to a threshold. The analysis allows for arbitrary spectra of information-bearing signal and noise processes. It yields two equations that relate five variables/parameters: the probability of false detection, the probability of missing a detection, window length, detection threshold, and signal-to-noise ratio (SNR). The probability density function of the detection variable is shown to be approximately Gamma distributed. All of the theoretical expressions and approximations are substantiated with simulation results.**

***Index Terms*—Burst detection, edge detection, energy detection algorithm, sliding window detector.**

I. Introduction

Energy detectors are commonly used to detect the presence of unknown signals [1]. The need for such detection can be found in many communication problems such as demodulation of ON–OFF keyed signals [2] and coarse timing acquisition in burst-mode orthogonal frequency division multiplexing (OFDM) [3], [4]. An energy detector measures the energy of the received signal over an observation time window and compares it with a predefined threshold to determine the presence of an information-bearing signal. Although it is not an optimum detector whenever the signal or noise is not a white Gaussian process, an energy detector is commonly used due to its simplicity.

The energy detection problem was first studied in [1] for *deterministic* signals transmitted over a flat band-limited Gaussian noise channel. The problem was revisited in [5] for signals transmitted over a variety of fading channels. More recently, [6] and [7] extended the analysis in [5] to include various receive diversity schemes.

This paper considers a similar energy-detection problem. In contrast to the previously mentioned related works, it does not restrict the noise to a flat bandpass spectrum. Moreover, the unknown signals are modeled as samples of a random process rather than being deterministic. While the analysis of such a model requires approximations, it is more reasonable in most communication applications since the information-bearing signal can take on many possible waveforms, depending on the random data sequence to be transmitted over the observation time window. The model, therefore, can also include the effect of the communication channel if its frequency response is known.

This paper develops two equations (approximations) that relate two performance measures to three design parameters. That is, they relate the probability of false detection and the probability of missing a detection to window length, detection threshold, and signal-to-noise ratio (SNR). While the approximations developed are not exact, they are very useful in determining the window length and the decision threshold.

Manuscript received July 27, 2007; revised January 17, 2008 and February 21, 2008. First published March 31, 2008; current version published November 12, 2008. This work was supported in part by Discovery Grants from the Natural Sciences and Engineering Research Council of Canada (NSERC). The review of this paper was coordinated by Dr. K. T. Wong.

The authors are with the Department of Electrical and Computer Engineering, University of Saskatchewan, Saskatoon, SK S7N 5A9, Canada (e-mail: eric.salt@usask.ca; ha.nguyen@usask.ca).

Digital Object Identifier 10.1109/TVT.2008.921617